SB^{3}C2017
Summer Biomechanics, Bioengineering and Biotransport Conference
June 21 – 24, Tucson, AZ, USA

Collagen Fiber Orientation of Tendon-Bone Insertion Tissues

Sandhya Chandrasekaran, Mark Pankow, Kara Peters, Hsiao-Ying Shadow Huang (1)

(1) Mechanical and Aerospace Engineering
North Carolina State University
Raleigh, NC, USA

INTRODUCTION: Tendon-bone insertion is a highly graded tissue, transitioning from 200MPa tensile modulus at the tendon end to 20MPa tensile modulus at the bone, across just a few hundred micrometers. In this study, we examine the insertion tissue macrostructure across its width and depth and provide a quantitative description of its collagen orientation and mineral concentration by using image analysis and mass spectrometry, respectively. Histological results revealed uniformity in global collagen orientation at all depths, indicative of mechanical anisotropy, although at mid-depth, the highest fiber density, least amount of dispersion, and least cellular circularity were evident. Collagen orientation distribution obtained through two-dimensional fast Fourier transformation (FFT) of histological imaging data from fluorescent microscopy agreed with past results based on polarized light microscopy. Results revealed global fiber orientation across the tendon-bone insertion to be preserved along physiologic tension. Gradation in the fiber distribution orientation index across the insertion was reflective of a decrease in anisotropy from the tendon to the bone.

The merit of this study lies in the image-based simplified approach to fiber distribution quantification and in the high spatial resolution of the compositional analysis. In conjunction with the mechanical properties of the insertion tissue, fiber and mineral distribution results for the insertion from the current study may potentially be incorporated into the development of a structural constitutive approach toward computational modeling. Characterizing the properties of the native insertion tissue would provide the microstructural basis for developing biomimetic scaffolds to recreate the graded morphology of a fibrocartilaginous insertion.

METHODS: Digital flexor tendon-bone units were removed from porcine forelimbs procured from the local abattoir. Two samples were preserved for microscopy in 10% buffered formalin under zero tension over two to three days prior to dehydration and decalcification. Specimens were processed for standard paraffin embedded histology and sectioned in both the horizontal and sagittal planes. Brightfield images at 400× magnification (water immersion) were obtained using the Zeiss Axioimager (Zeiss Inc., Germany) microscope at the Cellular and Molecular Imaging Facility at North Carolina State University. The collagen structures of both planes were imaged using Hematoxylin and Eosin (H&E) staining and Verhoeff-Van Geison (VVG) staining, respectively. For image analysis using fast Fourier transformation and utilizing the fluorescence of the dye, H&E stained sections at mid-depth in the horizontal plane were imaged using a GFP fluorescence filter set (excitation wavelength = 450-490 nm and emission wavelength = 500-550 nm) at a 40× objective (water immersion) (**Figure 1a**). Image analysis was performed after cropping out the three regions of interest, namely pure bone, insertion, and pure tendon, as shown in **Figure 1b** where α represents the mean fiber orientation in each image.

Images from fluorescent microscopy were converted from RGB to grayscale before converting to the frequency domain by applying 2D discrete Fourier transformation as shown in **Equation (1)** by using the function in a custom MATLAB (2016b, MathWorks, Natick, MA) script [1]:

$$F(u,v)=\sum_{x=1}^{M}\sum_{y=1}^{N} f(x,y)e^{-i2\pi(\frac{ux}{M})}e^{-i2\pi(\frac{vy}{N})} \qquad (1)$$

In **Equation (1)**, and denote the pixel coordinates on the image while and denote the frequencies corresponding to changes in the pixel intensity across the image spatial coordinates. Total pixel count is given by M×N for each of the cropped images in **Figure 1b**. For example, in the tendon region (T) the pixel count is 112×112. The simplistic case of

the regularly spaced alternating black and white stripes on an image would correspond to a single harmonic frequency. The actual image being analyzed is thus the inverse transformation of the superposition of such frequencies in the x and y-directions. The function is applied to the Fourier transform to cluster the zero-frequency component in the middle of the spectrum. The transform is converted to a log spectrum of its magnitude to eliminate its imaginary component. By means of noise filtering, the spectrum is shifted by its minimum value for the initial value to be zero and scaled down by its highest value to produce the FFT as shown in **Figure 1c**. The angle of orientation of white pixels on the FFT image is represented by Θ.

Fiber orientation distribution is interpreted based on the angular distribution of FFT image pixels. By fitting the FFT image pixel data onto a circular distribution, the number of pixels oriented along each incremental angle from 0 to π is obtained. The count of FFT image pixels associated with each incremental angle is baseline corrected using the minimum value and the result is normalized as a fraction of the maximum value. By numerical integration, the total area under angular distribution of the normalized pixel count is obtained. Each individual pixel count is further normalized by the total area to obtain the unit area orientation distribution as shown in **Figure 1d**. It should be noted that the orientation distribution corresponds to the angular orientation of the FFT image pixels with respect to the indicated coordinate system (**Figure 1c**). Mean angles of orientation associated with each of the three regions of interest are calculated as the angles corresponding to the centroids of the respective distributions. Hence, the peak angle in each distribution corresponds to the direction of highest frequency content and is presumably 90° out of phase with the orientation of the fibers in the cropped images in **Figure 1b**. For example, in the tendon region (T), the angle on the FFT (Θ) corresponding to a peak value of orientation distribution is 177° as seen in **Figure 1d**. This corresponds to a fiber orientation angle (α) of 87° (177° - 90° = 87°) in **Figure 1b**. Similarly, in the insertion region (I), the angle on the FFT (Θ) corresponding to a peak value of orientation distribution is 173° in **Figure 1d**. This corresponds to a fiber orientation angle (α) of 83° in **Figure 1b**. Orientation index (OI), used as a measure of fiber dispersion, is calculated as the difference between the angles bounding the middle 50% area under the orientation distribution curve. Hence, an increase in randomization of fiber direction would correspond to shorter peaks and wider orientation indices.

RESULTS

Fiber orientation gradation across insertion regions is studied quantitatively through image analyses of histological data as summarized in **Figure 1**. Fluorescent imaging (**Figure 1a**: H&E staining, GFP fluorescence filter set with excitation wavelength = 450-490 nm and emission wavelength = 500-550 nm, 40× objective, water immersion) was used to selectively crop out images from regions of interest, namely pure bone, insertion, and pure tendon, as shown in **Figure 1b**, and FFT was performed using a custom MATLAB code [1]. Results of FFT shown in **Figure 1c** clearly indicate gradation in the directionality of fiber orientation from the bone to the tendon region. Although the angle corresponding to peak values of orientation distribution is maintained across insertion, the progressive increase in the circularity of the FFT image from the tendon to the bony end is a reflection of the gradual decrease in the degree of anisotropy. This is in clear agreement with previous results from polarized light microscopy which also concluded that there is increased dispersion in fiber orientation at the bony end [2]. Angular distribution of FFT image pixels (indicated as Θ in **Figure 1c**) is obtained as a measure of the collagen fiber orientation distribution in each of the three regions of bone, insertion, and tendon, and the results are presented in **Figure 1d**. Thus, the orientation distribution of FFT at a given angle (Θ) indicates the associated number of frequencies in the frequency domain (or number of white pixels in the FFT oriented at Θ). The direction perpendicular to fiber orientation on the image would correspond to a higher number of associated frequencies and hence higher "orientation distribution." For example, in the cropped image from the tendon region in **Figure 1b**, the mean fiber direction (indicated as α) is oriented at nearly 177°. This indicates an angular orientation for the FFT at Θ = 87°. The orientation index predictably increases from the tendon to the insertion to the bone, suggesting a decrease in the directionality, i.e., decreases in the anisotropy of the fiber direction.

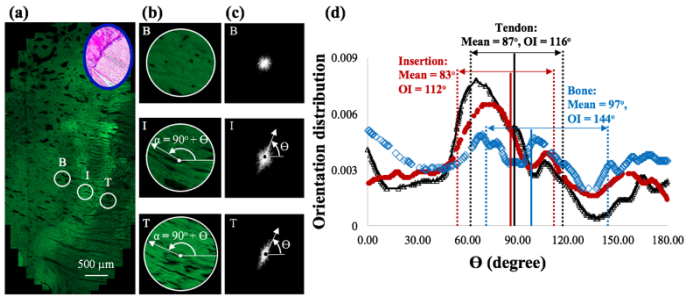

Figure 1 (a) H&E stained section was used for measurement of collagen fiber orientation in the bone (B), insertion (I), and tendon (T) regions. (b) Mean fiber orientation is represented by α in the cropped images, (c) FFT was applied to the cropped images. Angle of orientation of the white pixels on the FFT image is represented by Θ. (d) Orientation index decreases from bone to tendon, suggesting a decrease in fiber dispersion and an increase in anisotropy.

CONCLUSION

The insertion forms a functionally-graded interface between tendon and bone. This study addresses quantification of gradual changes in: (1) the orientation distribution of collagen fibers on two orthogonal planes; and (2) the relative concentration of the organic and inorganic tissue components. In this study, we have implemented an FFT-based method for determining collagen organization from histological sections which is shown to be an efficient replacement for the elaborate polarized light microscopy method. This quantification of collagen fiber orientation and dispersion across an insertion in the present study is validated against measurements from polarized light microscopy [3-4]. Features at the micrometer scale are important factors in the axial and shear moduli of tissue within the tendon-to-bone insertion [5]. Similar examination of the biocomposition across a healing tissue could help with understanding the contrast from results in a healthy tissue. The FFT provides complementary information about the complex structural properties of the inhomogeneous tendon-bone insertion tissue, and these results overall can pose important considerations in developing structure- and constituent-based constitutive models and injury mechanisms under super-physiological loading conditions.

ACKNOWLEDGEMENTS

This research was supported by NSF BMMB 1400018.

REFERENCES

[1] Masoumi N, Johnson KL, Howell MC, Engelmayr GC, Jr. Acta Biomater 2013;9(4):5974-88.

[2] Benjamin M, et al. Journal of Anatomy 1986;149:89-100.

[3] Thomopoulos S, et al. Journal of Orthopaedic Research 2003;21(3):413-419.

[4] Thomopoulos S et al. Journal of Biomechanics 2006;39(10):1842-1851.

[5] Genin GM, et al. Biophysical Journal 2009;97(4):976-985.